Tim-3 promotes cell aggressiveness and paclitaxel resistance through the NF-κB /STAT3 signaling pathway in breast cancer

Yizi Cong
Qindao University Medical College Affiliated Yantai Yuhuangding Hospital https://orcid.org/0000-0003-1349-6036

Yuxin Cui
Cardiff University

Shiguang Zhu
YANTAI YUHUANGDING HOSPITAL

Jianqiao Cao
Yantai yuhuangding hospital

Guangdong Qiao
Qindao University Medical College Affiliated Yantai Yuhuangding Hospital

Haidong Zou
Qindao University Medical College Affiliated Yantai Yuhuangding Hospital

Wenguo Jiang (jiangw@cardiff.ac.uk)

Zhigang Yu
Shandong University

Research

Keywords: breast cancer, Tim-3, tight junction, chemoresistance, aggressiveness.

Posted Date: June 12th, 2020

DOI: https://doi.org/10.21203/rs.2.22315/v2

Abstract

Background: T-cell immunoglobulin and mucin-domain containing molecule-3 (Tim-3) has been recognized as a promising target for cancer immunotherapy, but its exact role in breast cancer has not been fully elucidated.

Methods: The gene expression level of Tim-3 in breast cancer and its prognostic significance were analysed. In vitro functions and associated mechanisms were then explored through establishing Tim-3 overexpressing breast cancer cells.

Results: The gene expression level of Tim-3 was significantly higher ($p<0.001$) in breast cancer tissue compared to normal tissue following pooled analysis of TCGA database. Tim-3 was a prognosis indicator in breast cancer patients as shown by KM-plotter (RFS: $p=0.004$; OS: $p=0.099$). Overexpression of the Tim-3 in Tim-3^{low} breast cancer cells promoted aggressiveness of breast cancer cells including proliferation, migration, invasion, tight junction deterioration and tumour-associated tubal formation. Furthermore, Tim-3 enhanced cellular resistance to paclitaxel. Tim-3 exerted its function by activating the NF-κB/STAT3 signalling pathway, and mediating gene regulation (upregulating CCND1, C-Myc, MMP1, TWIST, VEGF while downregulating E-cadherin). Additionally, Tim-3 downregulated tight junction molecules: ZO-2, ZO-1 and Occludin, which might further facilitate the tumour progression.

Conclusions: Tim-3 plays a tumour-promoting role in breast cancer, which suggests targeting Tim-3 may acquire a clinical benefit in antitumor therapy.

1. Background

Breast cancer is the most frequently diagnosed malignancy and the main cause of cancer-associated mortality in women worldwide [1]. Although comprehensive treatments are clinically available, the response of individual breast cancer patients greatly varies, and partly due to their own different antitumor immunity [2]. Immune checkpoints play great roles in tumour immune evasion, especially by inducing tumour-reactive T-cell exhaustion [3]. For this reason, monoclonal antibodies against negative immune checkpoints such as programmed cell death protein 1 (PD1), have been used for the treatment of advanced triple-negative breast cancer (TNBC), and acquired some promising results [4].

T-cell immunoglobulin and mucin-domain containing molecule-3 (Tim-3), also known as hepatitis A virus cellular receptor 2 (HAVCR2), is a negative immune checkpoint molecule expressed on a variety of immune cells including T cells [5], dendritic cells [6], and macrophages [7]. Accumulating evidence demonstrate that Tim-3 can reduce cell proliferation, decrease the production of effective cytokines and increase apoptosis of effector T cells, through interaction with its ligands including galectin-9, high mobility group protein B1 (HMGB1), carcinoembryonic antigen related cell adhesion molecule 1 (CEACAM-1) and phosphatidylserine [8, 9].Tim-3 is now considered as a critical mediator in cancer progression and attracts considerable attention as a therapeutic target. Blocking Tim-3 indeed shows some promising results in multiple preclinical cancer models [10]. More importantly, there is evidence

suggesting that resistance to anti-CTLA-4 (cytotoxic T-lymphocyte-associated antigen 4) or anti-PD-1/PD-L1 inhibitors is partially by compensatory upregulation of additional immune checkpoints including Tim-3 [11]. And co-blockade of PD-1 and Tim-3 shows a significant survival advantage in a lung cancer mouse model [12]. These findings support the view that Tim-3 may be a potential target for tumour therapy.

Interestingly, Tim-3 is not only expressed on immune cells but also overexpressed on many types of malignant tumours. In vitro findings revealed that Tim-3 promoted metastasis of esophageal squamous cell carcinoma (ESCC) by inducing epithelial-mesenchymal transition (EMT) via the Akt/GSK-3/Snail signalling pathway. Tim-3 knockdown markedly inhibited proliferation, migration, and invasion of ESCC cell lines [13]. Additionally, Interfering Tim-3 expression can significantly suppress osteosarcoma cell proliferation and metastasis via the NF-κB/Snail signalling pathway and EMT [14]. Recently, a study in liver cancer indicated that tumour cell-intrinsic Tim-3 promotes cell proliferation via the NF-κB/IL-6/STAT3 cascade signalling axis [15]. Clinically, The ectopic expression of Tim-3 in tumour cells were correlated with more advanced pathologic T classification in non-small-cell lung carcinoma [16], lymph-vascular invasion in gastric cancer [17], lung metastasis in clear cell renal cell carcinoma [18], and lymphatic metastasis in colon cancer [9]. A meta-analysis revealed that higher expression of Tim-3 in solid tumours had significantly shorter overall survival [19]. Therefore, Tim-3 has been depicted as a prognostic indicator for those cancer patients. But contradictory results were also reported in terms of the role of Tim-3. Down-regulated Tim-3 promotes invasion and metastasis of colorectal cancer cells [20], and low expression level of Tim-3 in prostate cancer tissues is associated with poor prognosis for metastatic prostate cancer patients [21].Tim-3 expression either in primary or metastatic renal cell carcinoma is associated with longer progression-free survival (PFS) and overall survival (OS) [22]. The diverse prognosis significance of Tim-3 suggests that the role of Tim-3 might be dependent on tumour types or Tim-3 distribution.

Tim-3 is reported to be overexpressed in breast cancer tissues by limited immunohistochemistry analysis [19, 23], and high level of Tim-3 is associated with poor prognosis [23]. Downregulation or overexpression of Tim-3 lead to inhibited or promoted the proliferation, migration, and invasion of breast cancer cells, respectively [23]. However, the exact mechanisms of Tim-3 in breast cancer development and progression remain unknown. Additionally, previous studies showed Tim-3 was associated with resistance to anti-angiogenesis drug sunitinib and mTOR inhibitor rapamycin in a renal cell carcinoma cell line [24] , and induced chemoresistance to adriamycin and carboplatin in lymphoma ATN-1 cells [25], implying its possible role in tumour angiogenesis and chemoresistance. Therefore, in the present study, we first verified the clinical significance of Tim-3 by a large-scale genomic data analysis, and then evaluated the mechanisms underlying the effects of Tim-3 on cell proliferation, migration, and invasion in breast cancer cell lines. The role of Tim-3 in the tumor-associated angiogenic formation and chemo-drug response was also determined.

2. Methods

2.1 Cell lines and culture

The human breast cancer cell lines (MDA-MB-231 and MCF7) and human umbilical vein endothelial cells (HUVECs) were purchased from ATCC (Middlesex, UK). These cells were maintained in Dulbecco's Modified Eagle's Medium (DMEM/Ham's F-12 with L-Glutamine) (Sigma-Aldrich, Dorset, UK), supplemented with antibiotics (Sigma-Aldrich, Dorset, UK) and 10% fetal bovine serum (FBS) (Sigma-Aldrich, Dorset, UK). Cells were cultured at 37°C, 5% CO_2 in a humidified incubator.

2.2 Stable cell lines overexpressing Tim-3

To establish Tim-3 overexpressing breast cancer cell lines, the lentiviral vectors containing full length of Tim-3 (PLV [Exp]-EGFP: T2A: Puro-CMV> hHAVCR2 [NM_032782.4]) or Scramble (Scr) negative control (PLV [Exp]-EGFP: T2A: Puro-CMV>stuffer_300bp) were transduced into MDA-MB-231 and MCF7 cells respectively (Vector builder, USA) according to the manufacturer's instructions. Briefly, 5×10^4 cells were seeded into a 6-well plate overnight, and then subjected to medium containing 10 μg/ml polybrene and lentiviral particles. After incubation for 20 hours, the normal medium was applied for subsequent expansion for 3 days. Puromycin (Sigma, St. Louis, MO, USA) at a concentration of 2 μg/ml was used for stable cell selection. Following selection for one week, the stable cell lines were cultured in maintenance medium containing 0.25 μg/ml puromycin.

2.3 Quantitative real-time PCR（q-PCR）

Total RNA from cultured cells was extracted using TRIzol reagent (Sigma-Aldrich, Dorset, UK) according to the manufacturer's instruction. RNA was then reverse transcribed into cDNA using the GoScript™ Reverse Transcription System kit (Promega, Madison, WI, USA). Subsequently, quantitative real-time PCR was carried out using an iCycler iQ™ (Bio-Rad Laboratories, Hemel Hempstead, UK) following the cycling conditions: 94°C for 5 min, 100 cycles of 94°C for 10 sec, 55°C for 35 sec and 72°C for 20 sec. The primer sequences used in this study were listed in Table 1. Levels of mRNA were normalized to those of glyceraldehyde-3-phosphate dehydrogenase (GAPDH) using the $2^{-\Delta Ct}$ method.

Table 1. Primer sequences used in the qRT-PCR.

Gene	Forward Primers(5'-3')	Reverse Primers(5'-3')
CCND1	CGGTGTCCTACTTCAAATGT	**ACTGAACCTGACCGTACA**GAAGCGGTCCAGGTAGTTC
C-Myc	TGCTCCATGAGGAGACAC	**ACTGAACCTGACCGTACA**TGATCCAGACTCTGACCTTT
E-cadherin	CACACGGGCTTGGATTT	**ACTGAACCTGACCGTACA**GACCTCAAAAGGTACCACAT
GAPDH	CTGAGTACGTCGTGGAGTC	**ACTGAACCTGACCGTACA**CAGAGATGATGACCCTTTTG
IL-6	TCATCACTGGTCTTTTGGAG	**ACTGAACCTGACCGTACA**CAGGGGTGGTTATTGCATC
MMP1	CTTTTGTCAGGGGAGATCAT	**ACTGAACCTGACCGTACA**GGTCCACCTTTCATCTTCAT
NF-κB	ACAGAGAGGATTTCGTTTCC	**ACTGAACCTGACCGTACA**GTTGCAGATTTTGACCTGAG
Occludin	GAATTCAAACCGAATCATTG	**ACTGAACCTGACCGTACA**TGAAGAATTTCATCTTCTGG
STAT3	CATGGAAGAATCCAACAACG	**ACTGAACCTGACCGTACA**AATCAGGGAAGCATCACAAT
Tim-3	GCTCCATGTTTTCACATCTT	**ACTGAACCTGACCGTACA**ATTCCACTTCTGAGGACCTT
TWIST	AGCAACAGCGAGGAAGAG	**ACTGAACCTGACCGTACA**GAGGACCTGGTAGAGGAAGT
VEGFA	GAGCCGGAGAGGGAG	**ACTGAACCTGACCGTACA**CTGGGACCACTTGGCAT
VEGFD	TCCACATTGGAACGATCTGA	**ACTGAACCTGACCGTACA**CTCCACAGCTTCCAGTCCTC
ZO-1	TGACACACATGGTAGACTCA	**ACTGAACCTGACCGTACA**GTAACTGCGTGAATATTGCT
ZO-2	CAAAAGAGGATTTGGAATTG	**ACTGAACCTGACCGTACA**GAGCACATCAGAAATGACAA
β-catenin	AAAGGCTACTGTTGGATTGA	**ACTGAACCTGACCGTACA**CTGAACTAGTCGTGGAATGG

Note: Z Sequence 'ACTGAACCTGACCGTACA' is highlighted in bold font.

2.4 Western blotting

Cells grown in culture flasks were detached and lysed using a protein lysis buffer. Protein concentration was determined by a Bio-Rad DC protein assay kit (Hemel-Hempstead, UK). Equal amounts of protein samples were separated using sodium dodecyl sulphate-polyacrylamide gel electrophoresis (SDS-PAGE) and blotted to PVDF membrane. The membrane was then blocked using 5% skimmed milk for 2 hours. Proteins were then probed with a primary antibody and a corresponding peroxidase-conjugated secondary antibody. The stained protein bands were visualized using Luminata Forte Western HRP substrate (Merck Millipore, Hertfordshire, UK) and analysed using the ImageJ software (National Institutes of Health, Bethesda, MD, USA) by densitometry.

The antibodies of Tim-3 (Ab241332), NF-κB (p65) (Ab16502), p-NF-κB (p-p65) (Ab194726) and VEGFA (Ab9570) were purchased from Abcam (Cambridge, UK). GAPDH (sc-47724), p-β-catenin (sc-16743-R), CCND1 (sc-8396), C-Myc (sc-70465), MMP1 (sc-21731), TWIST (sc-6269), ZO-1(sc-10804), ZO-2(sc-11448), Occludin (sc-133256) and VEGFB (sc-13083) antibodies were purchased from Santa Cruz (Insight Biotechnology Limited, Middlesex UK). E-Cadherin (AF748) and VEGFD (MAB286) antibodies were purchased from R & D Systems (Abingdon, Oxfordshire, UK). STAT3 (S5933), p-STAT3 (SAB4504541), IL-6(17901) and β-catenin (C2206) antibodies were purchased from Sigma-Aldrich (Gillingham, Dorset, UK). Anti-mouse (A5278), anti-rabbit (A0545) and anti-goat (A8919) secondary antibodies were obtained from Sigma-Aldrich (Gillingham, Dorset, UK).

2.5 Cell proliferation and cytotoxicity assay

Cell proliferation was assessed by AlamarBlue assay. Briefly, cells at a density of 3×10^3 cells/well were seeded into a 96-well plate and incubated at 37°C, 5% CO_2 for 6 days. The medium was changed every 3 days during this period. At each designated time point (Day 0, 2, 4 and 6), the medium was aspirated and 100 µl of fresh medium containing 10 µl of AlamarBlue reagent (Serotec Ltd., Oxford, UK) was added to each well. Cells were then incubated for 3 hours at 37˚C. The fluorescence was measured using a fluorescence plate reader (Promega, Southampton, UK) with excitation at 525 nm and emission at 590 nm. The percentage of growth during the incubation period was then calculated against the fluorescence values at Day 0.

For cytotoxicity assay, 8×10^3 cells per well were seeded into a 96-well plate in the medium containing 1% FBS. After cells were starved overnight, medium was replaced with different concentrations of paclitaxel (Sigma-Aldrich, UK) and treated for 48 h, cell viability was then assessed by AlamarBlue assay as described above.

2.6 Scratch wound assay

Cells were seeded into a 24-well plate at a density of 2×10^5 cells/well and grown to reach confluence. The cell monolayer was then scratched using a 1 ml pipette tip to generate an artificial wound. After washed twice with phosphate buffered saline (PBS), Normal medium was added with 1 ml per well. Migration of cells to wounding gap was monitored by an EVOS® FL imaging system (Life technologies, Carlsbad, CA, USA) with a 4X objective every 2 hours for 24-48 hours. The percentage of closed area in the wounding gap was measured and normalized using the data from 0 h using ImageJ software.

2.7 Matrigel invasion assay

A transwell Matrigel assay was used to assess the invasive ability of cells *in vitro*. Briefly, transwell inserts (8 µm pore size) for a 24-well plate were pre-coated with 100 µl of 0.5 mg/ml Matrigel (BD Bioscience, Oxford, UK) for 1 h at 37˚C. Subsequently, 2×10^4 cells (MDA-MB-231) or 2×10^5 cells (MCF7) were seeded into each upper chamber in 150 µl plain medium, and 650 µl normal medium was added to the lower chamber. After incubation for 48 h, cells on the top side of inserts were removed with a cotton

swab. Chambers were then fixed with 4% formalin for 30 mins, and stained with 1% crystal violet for 30 mins before rinsing with PBS. The numbers of invasive cells (cells under the inserts) were determined by counting under a microscope (at least five counts per experimental setting).

2.8 Cell-matrix adhesion assay

A 96-well plate was coated with Matrigel (10 μg/well) for 2h at 37°C to allow extracellular matrix protein binding to the cell culture surface. Cells at a density of 2×10^4 cells/well were added and incubated for 1 h, followed by washing with PBS twice. Adhesive cells were then fixed with 4% formalin and stained with 1% crystal violet before rinsing with PBS. The number of attached cells was determined by counting under a microscope (at least five counts per experimental setting).

2.9 Tube formation assay mediated by tumor conditioned medium

Stable cancer cells containing Tim-3 overexpression or Scr control vectors were cultured to reach 70-80% confluency in complete medium. Medium was then replaced with serum-free medium after washed twice with PBS. The supernatant (conditioned medium) was then collected after cultured for 24 h, filtered with a 0.22μm filter (Millipore) and stored at -80˚C for further use. HUVECs were used for tube formation after three to four passages. A pre-chilled 96-well plate coated with a thin layer of the Matrigel (50 μl/well) was incubated to polymerize at 37°C for 1 h. 2×10^4 HUVECs resuspended in 200 μl conditioned medium were seeded to each well and incubated at 37°C, 5% CO_2 for 16 h. Five random views were chosen to evaluate tube formation ability by counting the total segment length using ImageJ software.

2.10 Electric cell-substrate impedance sensing (ECIS) assay

The ECIS assay was employed to assess cell migration as described previously [26]. Briefly, The ECIS Zθ system with a 96W1E+ array plate (Applied Biophysics, Inc., Troy, NY, USA) was applied for the measurement of cell functions including initial attachment, spreading and tight junction (TJ) of the cells. The 96W1E+ array plate was stabilized using the normal medium for 2 h in advance. 5×10^4 cells per well were then seeded and cultured for 24 hours. Each group was set up at least six repetitions. The resistance across the array was recorded at multiple frequencies by the system.

2.11 Transepithelial resistance (TER) and paracellular permeability (PCP)

TER was used to assess the integrity of tight junction dynamics in cell culture models of epithelial monolayers as a widely accepted quantitative technique. An EVOM voltohmmeter (World Precision Instruments, Aston, Herts, UK), equipped with STX2 chopstick electrodes (World Precision Instruments, Inc., Sarasota, FL, USA) was used to measure the TER. Briefly, 5×10^4 cells were seeded into a 0.4 μm pore size insert (Greiner Bio-One Ltd, Stonehouse, UK) and allowed to reach full confluence. Following the replacement with fresh medium, electrodes were placed at the upper and lower chambers and resistance were measured with the Volt-Ohm meter. Inserts containing cell-free medium were set as blank control. After TER was recorded, the medium in upper chamber was replaced with normal medium containing 0.2

mg/ml fluorescein isothiocyanate (FITC)-dextran 10 kDa. 50 µl of medium from outside of the insert was transferred into a black 96-well cell culture microplate (Greiner Bio-One) in duplicate every 2 hours for 10 hours. Basolateral dextran passage was analysed with a GloMax®-Multi Microplate Multimode Reader (Promega UK Ltd., Southampton, UK) at excitation 490nm and emission 510-570nm. Measurement of dextran-indicated PCP was then normalized to the 0 h via subtraction.

2.12 Statistical analysis

Data values are presented as mean ± SD unless stated otherwise. GraphPad Prism (Version 7.0, GraphPad Software, San Diego, CA) or R language (version 3.6.3. https://www.R-project.org) were used for statistical analysis. Two-group comparisons were analysed using two-sided t-test when data were normally distributed or Mann-Whitney U test when not normally distributed. For multiple groups, if data passed a Shapiro-Wilk normality test, their differences were then analysed using ANOVA followed by the post hoc Tukey HSD test for pairwise comparison; otherwise, the Kruskal-Wallis test was used. Differences were considered statistically significant when p-values were less than 0.05. Experiments were repeated 2-4 times unless otherwise stated. The statistical significance in the figures was shown as follows: *p<0.05; **p<0.01; ***p<0.001.

3. Results

3.1 Tim-3 is upregulated in breast cancer tissues

Firstly, we analysed the gene expression level of Tim-3 in breast cancer and normal tissues in the TCGA BRCA datasets. The analysis indicated that Tim-3 was significantly overexpressed in breast cancer (n=1097) compared with normal tissues (n=114) (p<0.001) (Fig.1A). There was no statistical difference among different subtypes of breast cancer (p=0.074) (Fig.1B). We further investigated its survival significance from the analysis of KM-plotter database (http://kmplot.com/analysis/) through entering ‘Gene symbol= HAVCR2 (235458_at)’, selecting ‘JetSet best probe set’, and splitting patients by ‘Auto select best cutoff ’. It showed that the patients with a high level of Tim-3 had a significantly worse relapse-free survival（RFS）when followed up for more than 20 years (p=0.004) (Fig. 1C). The overall survival (OS) had a similar trend but there was no statistical significance (p=0.099) (Fig. 1E). For subgroup analysis, the high expression level of Tim-3 was associated with worse RFS in Luminal A (p<0.001) and luminal B (p=0.039) subtypes, while on the contrary, with better RFS in basal breast cancer (p<0.001) (Fig.1D). HER2 positive subtype had a similar trend with basal subtype but without statistical significance (p=0.12) (Fig.1D). For OS, high level of Tim-3 was associated with worse prognosis in luminal A subtype (p=0.019), while in basal type, patients with high level of Tim-3 had a better prognosis (p<0.001) (Fig.1F). We also analysed the possible effect of adjuvant treatments on the RFS, as shown in the Sup. Fig. 1, the RFS pattern of Tim-3 was reversed in those patients with chemotherapy (p=0.0036, HR=0.56, n=366), which is particularly the case in those with adjuvant treatment (p=0.0054, HR=0.52, n=255).

3.2 Stable cell lines overexpressing Tim-3

In order to evaluate the role of Tim-3 in breast cancer *in vitro*, MDA-MB-231 and MCF7 cell lines with the low level of Tim-3 expression (initial assessment shown in Sup.Fig.2) were stably transfected with full-length Tim-3 expressing plasmid or empty vector (Scr) as controls, respectively. After transfection, the expression level of Tim-3 was assessed by q-PCR and Western blot. As shown in figure 2A, Tim-3 levels were dramatically increased in the Tim-3 overexpression cell lines (Tim3 OE) compared with the Scr and wildtype (WT) controls at both mRNA and protein levels, which confirmed Tim-3 was successfully transfected into these two cell lines. We also performed an IHC assay to visualize the expression of Tim-3 protein in cells and found that Tim-3 was expressed in both cell cytoplasm and membrane after stable overexpression (Sup.Fig.3).

3.3 Effect of Tim-3 in cell proliferation and adhesion *in vitro*

We then attempted to determine the role of Tim-3 in cell proliferation and adhesion *in vitro*. The proliferation data demonstrated that both MDA-MA-231 Tim3 OE and MCF7 Tim3 OE cells have an increased capability of cell growth compared with their Scr controls especially when cultured for 6 days ($p < 0.001$, respectively) (Fig.2B, 2C), which indicated that Tim-3 could promote breast cancer cell proliferation. Cell-matrix adhesion assay was used to investigate the role of Tim-3 in cell adhesion. As shown in Fig.2E, the adhesive ability of cells was increased when Tim-3 was overexpressed in MCF7 cell line ($p<0.001$). On the contrary, Tim-3 overexpression reduced the adhesive ability in the MDA-MB-231 cell line ($p=0.006$) (Fig.2D), which suggested that the effect of Tim-3 might be cell type dependent.

We then examined the signalling pathways in Tim3 OE breast cancer cells based on previous studies. We found that NF-κB (p65), STAT3 and IL-6 were all upregulated both at gene and protein levels in MDA-MB-231 Tim3 OE cells. Also, the p-STAT3 level was increased in MDA-MB-231 Tim3 OE cells (Fig.2F and 2G). NF-κB (p65), p-NF-κB (p-p65), STAT3, p-STAT3 and IL-6 were also upregulated in MCF7 Tim3 OE cells at protein level (Fig.2F and 2G). Moreover, cell proliferative proteins including β-catenin, p-β-catenin, Cyclin D1 and C-Myc were upregulated in MDA-MB-231 Tim3 OE cells (Fig. 2G), which were confirmed by q-PCR (Fig.2H). β-catenin, p-β-catenin and C-Myc were also increased in MCF7 Tim3 OE cells at protein level(Fig. 2G) but not at gene level (Fig.2I). These findings supported that NF-κB/ STAT3 pathway was involved in breast cancer progression when Tim-3 was upregulated.

3.4 Tim-3 increases cell invasion and migration in vitro

In order to characterize the effects of Tim-3 on cell invasion and migration, we performed Matrigel transwell invasion assay and wound healing assay. Matrigel invasion assay revealed that Tim3 OE cells were significantly more invasive than the Scr controls both in MDA-MB-231($p=0.030$) (Fig.3A) and MCF7 ($p<0.001$) (Fig.3B) cells. Wound healing assay demonstrated that cell migration ability was also enhanced in MDA-MA-231 Tim3 OE (24h, $p<0.001$) (Fig.3C) and in MCF7 Tim3 OE cells (48h, $p=0.007$) (Fig.3D), respectively. We further detected EMT associated molecules considering that EMT was a key step in tumour metastasis. Indeed, we demonstrated that Tim-3 downregulated the epithelial marker E-cadherin but upregulated an EMT trigger TWIST in both MDA-MB-231 and MCF7 cells (Fig.3E) at the protein level. As a downstream target of TWIST, MMP1 was also dramatically upregulated in MDA-MB-

231 Tim3 OE cells at the protein level (Fig.3E). We also observed the upregulation of TWIST and downregulation of E-cadherin in MCF7 Tim3 OE cells at gene level (Fig.3F). These findings suggested that EMT indeed facilitated the invasion of Tim-3 overexpressing cells in breast cancer.

3.5 Tim-3 disrupts TJ integrity

TJ constitutes a fundamental complex structure that cancer cells need to destroy in order to metastasize. We herein evaluated the role of Tim-3 in TJ function of breast cancer cells. ECIS was firstly used to evaluate the resistance at 1kHz as the current at this frequency is mainly flowing outside of the cell and therefore is representative of cellular interactions. The ECIS results showed that Tim3 OE cells have lower resistance in comparison to scramble cells during initial attachment and spreading in MDA-MB-231 and MCF 7 cell lines (Fig.4A), which implied Tim-3 might deteriorate the function of cell-cell TJ.

To verify the initial findings by ECIS, we performed the TER and PCP assays to examine the effect of Tim-3 on TJ barrier function. As displayed in figure 4B, TER values in Tim3 OE cells were reduced in comparison to the Scr controls in both MDA-MB-231($p<0.001$) and MCF7 ($p<0.001$) cells. In parallel with TER, the PCP governed by TJs between polarized cells monolayers was assessed using FITC dextran 10 kDa as a tracer. Results showed a higher PCP fluorescence signals in Tim3 OE cells than in Scr cells from both MDA-MB-231(10h, $p=0.002$) and MCF7 (10h, $p=0.023$) cell lines (Fig.4B), which further confirmed that Tim3 OE cells had a looser connection of cell-cell junctions.

There is evidence that the expression or distribution of TJ proteins is usually altered in cancer, while most cell-cell adhesion proteins are downregulated and others may be overexpressed or dyslocalized. We, therefore, investigated the alteration of the key TJ molecules in cancer cells after Tim-3 overexpression. We observed that ZO-2 was reduced in both MDA-MB-231 and MCF7 Tim3 OE cells at protein level (Fig.4D and 4E), the gene level of ZO-2 was also downregulated in MDA-MB-231 Tim3 OE cells (Fig.4F). The protein level of ZO-1 was downregulated in MDA-MB-231 Tim3 OE cells, and Occludin was downregulated in MCF Tim3 OE cells. These results indicated that Tim-3 disrupt the TJ integrity through regulating the expression of TJ proteins.

3.6 Tim-3 promotes tube formation of endothelial cells

To explore whether Tim-3 plays a role in mediating tumor-associated angiogenesis, tube formation assay was performed using endothelial cells subjected to conditioned medium from stable cells with Tim-3 overexpression. As shown in Fig.5A, the tube formation ability of HUVECs cultured in medium from MDA-MB-231 Tim3 OE cells was significantly increased when cultured for 8 hours ($p=0.014$), the similar phenomenon was also observed in medium from MCF7 Tim3 OE cells when cultured for 16 hours ($p=0.016$) (Fig.5B), which indicated that overexpression of Tim-3 was involved in promoting tumour-associated angiogenesis.

To investigate whether the role of Tim-3 in tumour-associated angiogenesis was VEGF dependent, we evaluated the levels of VEGF family proteins using Western Blot. As shown in Fig.5C, the protein levels of

VEGFA, VEGFB and VEGFD were all increased in MDA-MB-231 Tim3 OE cells, while the protein level of VEGFA was increased in MCF7 Tim3 OE cells. However, gene expression analysis indicated that the level of VEGFD was increased in MCF7 Tim3 OE cells (Fig.5D). We evaluated the extracellular levels of VEGFC and VEGFR2 proteins by ELISA. The ELISA data indicated that VEGFC was significantly increased in the MDA-MB-231 Tim3 OE cells ($p<0.01$) compared to the Scr control (Sup. Fig. 5). The difference of VEGFC in the MCF7 cell lins was also significant but the overall levels of VEGFC in MCF7 cells were extremely low compared to MDA-MB-231 although there is significance ($p<0.05$). The extracellular levels of VEGFR2 had no significance in the MDA-MB-231 cells or were low in the MCF7 cells. These results implied there is VEGF dependency in Tim-3 mediated angiogenesis.

3.7 Tim-3 enhances breast cancer cell resistance to paclitaxel

In order to evaluate the role of Tim-3 in chemo-drug sensitivity in breast cancer, MDA-MB-231 and MCF7 cells were treated with different concentrations of paclitaxel before their viability was assessed by AlamarBlue assay. As shown in figure 6A and 6C, MDA-MB-231 Tim3 OE cells were more resistant to paclitaxel than the scramble cells at concentrations of 10 nM ($p=0.049$), 20 nM ($p=0.003$) and 40 nM ($p<0.001$). MCF7 Tim3 OE cells were also more resistant to paclitaxel at concentrations of 2.5 nM ($p=0.043$) and 5 nM ($p=0.002$) rather than higher concentrations compared to the Scr control.

We further demonstrated the level alteration of the STAT3, NF-κB, p-NF-κB, and CCND1 proteins by Western blot after cells were treated with single-dose paclitaxel (10 nM for MDA-MB-231 and 5 nM for MCF7) for 6h and 24h, respectively. We found that the level of total NF-κB protein was significantly higher in Tim3 OE cells when cultured for 6 hours, and p-NF-κB was significantly higher in Tim3 OE cells when cultured for 24 hours in both cell lines compared to the Scr controls (Fig.6B and 6D). After paclitaxel treatment for 24 hours, the protein levels of STAT3 were significantly higher in Tim3 OE cells than Scr cells in both cell lines. The level of CCND1 in MCF7 Tim3 OE cells was significantly higher than control cells when cultured for 6 hours (Fig 6B and 6D). To validate the function involvement of NF-κB and STAT3 in the Tim-3 mediated paclitaxel resistance, we performed cytotoxicity assay using NF-κB inhibitor (SC75741) or STAT3 inhibitor (Stattic). As shown in the Sup. Fig. 4, in the presence of either SC75741 Stattic, the paclitaxel resistance induced by Tim-3 was abolished. The data, therefore, provided evidence that the NF-κB and STAT3 activities were involved in Tim-3 mediated paclitaxel resistance.

4. Discussion

In recent years, targeting immune checkpoints in breast cancer, especially in TNBC, has attracted accumulating interest to overcome the lack of efficacy of any targeted therapy. Emerging reports unveil the endogenous functions of Tim-3 in regulating the immune response during cancer progression. As a negative immune regulator, Tim-3 has also been proposed as a prognostic indicator in several types of solid tumours [19].

Previous small-scale studies suggest that Tim-3 is overexpressed in breast cancer. Positive Tim-3 staining in breast cancer is significantly higher than adjacent tissues as shown by immunohistochemistry

(n=42) [23], Tim-3 expression in invasive ductal breast carcinoma cells is also significantly higher than that in normal breast tissues [19]. The gene expression level of Tim-3 is also reported to be higher in breast tumour tissues (n=8) [27]. Moreover, high level of Tim-3 is correlated with more advanced clinical stage, lymph node metastasis, higher Ki67 and a poorer 5-year patient survival rate [19, 23]. Our results from the pooled analysis of the large-scale TCGA and KM-plotter databases further confirm that Tim-3 expression is indeed upregulated in breast cancers and is associated with a poor prognosis in overall survival, which is in accordance with previous studies.

To determine the biological functions of Tim-3 in breast cancer, we established the stable Tim-3 overexpressing breast cancer cell lines using wild-type MDA-MB-231 and MCF7 cells. Using these in-vitro cell models, we demonstrate that Tim-3 promotes the aggressiveness properties of cells including proliferation, migration and invasion.

It has been reported that the signalling of Tim-3 is associated with the downstream effector NF-κB in negative regulation of T cell function or liver cancer [28-30]. NF-κB plays a key role in targeting the IL-6/STAT3 axis which is involved in the pro-tumor activity [31]. We, therefore, examined the levels of Tim-3 associated signalling pathway checkpoints including NF-κB, STAT3 and IL-6 as a consequence of Tim-3 overexpression. It turns out that NF-κB, STAT3 and IL-6 are all upregulated as a response to Tim-3 overexpression, which implies that these molecules were involved in the functions of Tim-3 in breast cancer cells. In a similar manner, a recent study in liver cancer also demonstrates that Tim-3 overexpression enhances tumour cell growth by activating the NF-κB/IL-6/STAT3 pathway axis, while Tim-3 inhibition results in suppressed tumour growth both in vitro and in Tim-$3^{knockout}$ mice [15]. Another study using clear cell renal carcinoma cell lines also shows that knockdown of Tim-3 leads to the suppression of the tumor cell proliferation and invasion [18], which indirectly supports our findings.

STAT3 has been initially discovered to bind to DNA after phosphorylation in response to IL-6 and epidermal growth factor [32]. The level and activity of STAT3 have been linked with cancer initiation, progression, metastasis, chemoresistance and immune evasion [33]. STAT3 has been widely recognized as a multi-functional oncogenic factor with novel therapeutic target potential [34, 35]. The recent advances from both preclinical and clinical studies suggest that STAT3 plays a critical role in breast cancer and STAT3 inhibitors do show efficacy in inhibiting TNBC tumour growth and metastasis [36]. Besides regulating downstream gene expression in its phosphorylated state, STAT3 may also be involved in transcriptional regulation by forming complexes with NF-κB in its unphosphorylated form [37]. The cooperation of STAT3 and NF-κB has also been reported in fascin expression that accelerates the migration of breast cancer cells [38]. STAT3 signalling promotes breast tumour progression through regulating its downstream molecules which control cell proliferation (by CCND1, C-Myc, Bcl-2, Bcl-xL and Survivin), angiogenesis (by HIF1α and VEGF) and epithelial-mesenchymal transition (by TWIST, Vimentin, MMP9 and MMP7) [39]. In our present study, CCND1and C-Myc are both upregulated in Tim-3 overexpressing cells, through which to facilitate cell proliferation. Previous studies have provided evidence that there is a positive correlation between STAT3 and CCND1 in both primary breast tumours and breast cancer cell lines [40]. To control cell cycle progression from G1, CCND1 assembles with the

cyclin dependent kinases 4/6 (CDK4/6), phosphorylates substrates such as retinoblastoma protein (Rb), releases E2F transcription factor and promotes entry of cells to the S-phase [40]. As a proto-oncogene, C-Myc is known to be associated with the high grade and the advanced stage of TNBC, and correlates with poor prognosis [41]. Based on the evidence as above, we propose that Tim-3 upregulates CCND1 and C-Myc by activating STAT3, which eventually promotes cell proliferation in breast cancer.

Distant metastasis is the leading cause of cancer-related death in breast cancer patients. In our study, Tim-3 is found to promote the capacities of cell invasion and migration, implying its potential role in cancer metastasis. EMT is a key process during cancer invasion and metastasis, which confers an aggressive phenotype to tumour cells. Our study shows that Tim-3 overexpression has an influence on the EMT associated molecules. Tim-3 overexpression significantly elevates the level of MMP1 in MDA-MB-231 cells, while downregulates E-cadherin and upregulates TWIST in both MDA-MB-231 and MCF7 cells. It has been reported that there is a positive correlation between phosphorylated STAT3 and TWIST in primary breast carcinoma [42]. Therefore, we speculate that Tim-3 promotes breast cancer invasive ability by regulating STAT3 and its downstream EMT-associated molecules, which in complying with a previous study in human osteosarcoma [43].

Loss or reduction of intercellular adhesion molecules also facilitates tumour cells detachment from primary tumours, ultimately initiating metastasis. In this study, we identify that Tim-3 disrupts the cell-cell tight junction integrity through downregulating the tight junction molecules including ZO-2, ZO-1 and Occludin. ZO-2 and ZO-1 belong to the membrane-associated guanylate kinase protein family and interact with a wide variety of molecules, including cell-cell adhesion proteins, cytoskeletal components and nuclear factors [44]. A previous study reveals that STAT3 activation induced by IL-6 increases the retinal endothelial permeability and vascular leakage through the reduction of ZO-1 and Occludin expression [45]. STAT3 also suppresses CLDN1 transcription by direct binding to its promoter [46, 47]. VEGF is also able to induce the phosphorylation and downregulation of ZO-1 and ZO-2 in endothelial cells [48]. In addition, VEGF promotes motility and reduces the expression of ZO-2 in pancreas cancer cells [49]. Based on our findings and previous reports, we speculate that Tim-3 promotes the ability of invasion and migration partially by disrupting the cell-cell tight junction through downregulating ZO-2, ZO1 and Occludin, which maybe STAT-3 and VEGF dependent.

It has been reported that Tim-3 promotes the resistance to the anti-angiogenesis drug sunitinib and mTOR inhibitor rapamycin in renal cell carcinomas cell line [24], implying its possible effect on tumour angiogenesis. Sunitinib inhibits angiogenic signalling pathways by targeting multiple receptor tyrosine kinases (RTKs) including platelet-derived growth factor (PDGF) and vascular endothelial growth factor receptors (VEGFRs). Therefore, we attempted to determine the potential role of Tim-3 in endothelial cell tube formation. Interestingly, our data indicate that conditioned medium from Tim-3 overexpressing cancer cells accelerates tube formation compared with the controls in both MDA-MB-231 and MCF7 cell lines. To understand whether Tim-3 mediated tube formation is VEGF dependent, we evaluated the expression levels of VEGF family in the stable cell lines with Tim-3 overexpression. We demonstrate that the levels of VEGFA, VEGFB and VEGFD were all increased in MDA-MB-231 Tim3 OE cells, while the level

of VEGFA was increased in MCF7 Tim3 OE cells. Previous studies reveal that STAT3 plays an important role in angiogenesis. For instance, STAT3 and HIF1α cooperatively activate VEGF and haptoglobin (Hp) genes during hypoxia in breast cancer cell lines [50], which may also partially contributes to the role of Tim-3 in promoting angiogenesis.

Chemoresistance has been a major obstacle in treating breast cancer, especially for TNBC. As a first-line chemotherapeutic reagent for metastatic breast cancer, paclitaxel acquires a high drug response rate. However, there is a high frequency of patients acquiring resistance but the underneath mechanism remains poorly understood. A previous study shows that Tim-3 overexpression induces chemoresistance to adriamycin and carboplatin in lymphoma ATN-1 cells [25]. The Tim-3 expression is increased in patients with head and neck squamous cell carcinoma after combinational chemotherapy (docetaxel, cisplatin and fluorouracil) or pre-radiotherapy [51]. And a Tim-3 antibody is able to improve the response to paclitaxel in models of triple-negative and luminal B breast cancer [6]. All these previous studies suggest a role of Tim-3 in chemotherapeutic resistance in cancer. In our study, we find that Tim-3 overexpression in breast cancer cells is more resistant to paclitaxel, which could be due to the upregulation of STAT3 and NF-κB. Considerable studies have confirmed the role of STAT3 in cancer chemoresistance. For example, paclitaxel induces apoptosis in human ESCC cell lines (EC-1 and Eca-109 cells) through the reduction of total STAT3 and phospho-STAT3 proteins [52]. Also the tumor cell sensitivity to paclitaxel can be improved by the targeting of STAT3 using micro RNAs such as miR-125a and miR-29a [53, 54]. Also in the lung adenocarcinoma cells, resistance to paclitaxel positively correlates with STAT3 activation and the autocrine production of IL-6 through a positive-feedback loop [55]. Therefore, it is possible that Tim-3 enhances paclitaxel resistance by upregulating STAT3 in breast cancer, which implying its potential value in predicting drug response.

As indicated by the analysis of KM-plotter database, although Tim-3 is associated with poor prognosis in total breast cancer patients, the prognostic significance is varied in different subtypes. High-level expression of Tim-3 is associated with poor RFS in Luminal A and luminal B subtypes, while on the contrary, with better RFS in basal breast cancer. Our study shows that both MCF7 and MDA-MB-231 cells exhibited a more malignant phenotype after Tim-3 overexpression, which might be associated with poor prognosis in vivo. Two recent studies, however, suggest that Tim-3^+ tumor-infiltrating lymphocytes (TILs) correlates with hematoxylin and eosin-stained TILs and is associated with better DFS and OS based on the analysis of 3,992 breast cancer specimens [56] including 109 samples of TNBC [57]. We therefore speculate that the distribution of Tim-3 expression on tumour cells or immune cells might have different prognostic significance, and the major location of Tim-3 in certain types of cells in cancer might determine the prognostic outcomes, although advanced investigation including in vivo animal models would be required to unveil the paradox of the Tim-3 clinical significance in future.

Taken together, this study reveals that overexpressing Tim-3 in breast cancer not only promotes tumour cells proliferation, migration and invasion, but also disrupts the tight junction function, increases tumor-associated tube formation and paclitaxel-resistance. Tim-3 plays its role by activating the NF-κB/STAT3 signalling pathway and altering gene transcription including upregulating CCND1, C-Myc, MMP1, TWIST,

VEGF and downregulating E-cadherin. Moreover, Tim-3 modulates the dynamics and functions of the tight junction by downregulating the levels of ZO-2, ZO-1 and occludin, which may, in turn, facilitate tumour invasion and migration (as illustrated in Fig.7). Our findings suggest that Tim-3 may serve as a prognostic predictor or have therapeutic potential for breast cancer treatment.

Abbreviations

TNBC: advanced triple-negative breast cancer; Tim-3: T-cell immunoglobulin and mucin-domain containing molecule-3; HAVCR2: hepatitis A virus cellular receptor 2; EMT: epithelial-mesenchymal transition; PFS : progression-free survival; OS: overall survival; GAPDH: glyceraldehyde-3-phosphate dehydrogenase; SDS-PAGE: sodium dodecyl sulphate-polyacrylamide gel electrophoresis; PBS: phosphate buffered saline; ECIS: cell-substrate impedance sensing; TER: Transepithelial resistance; PCP: paracellular permeability; TJ: tight junction ; ESCC: esophageal squamous cell carcinoma.

Declarations

Availability of data and materials

All data generated or analysed during this study are included in this published article. The primary data that support the findings of this study are available from the corresponding authors upon reasonable request.

Conflict of interest

The authors declare no conflict of interest.

Funding

This study was supported by the key project of research and development plan of Shandong province (No.2018GSF118125) and Yantai city (No.2017YD007), and Cancer Research Wales.

Authors' contributions

WGJ, ZGY, YXC and SGZ conceived and planned the experiments. YZC and JQC carried out the experiments. GDQ and HDZ contributed to the interpretation of the results. YZC took the lead in writing the manuscript in consultation with YXC and ZGY. All authors provided critical feedback and helped shape the research, analysis and manuscript. All authors read and approved the final manuscript.

Acknowledgements

The authors thank the technical assistance from the members of the Cardiff China Medical Research Collaborative, UK.

Ethics approval and consent to participate

Not applicable.

Consent for publication

Not applicable.

Competing interests

The authors declare that they have no competing interests.

References

1. Bray F, Ferlay J, Soerjomataram I, Siegel RL, Torre LA, Jemal A: Global cancer statistics 2018: GLOBOCAN estimates of incidence and mortality worldwide for 36 cancers in 185 countries. CA: a cancer journal for clinicians 2018, 68:394-424.
2. de la Cruz-Merino L, Chiesa M, Caballero R, Rojo F, Palazon N, Carrasco FH, Sanchez-Margalet V: Breast Cancer Immunology and Immunotherapy: Current Status and Future Perspectives. Int Rev Cell Mol Biol 2017, 331:1-53.
3. Fuertes Marraco SA, Neubert NJ, Verdeil G, Speiser DE: Inhibitory Receptors Beyond T Cell Exhaustion. Front Immunol 2015, 6:310.
4. Schmid P, Adams S, Rugo HS, Schneeweiss A, Barrios CH, Iwata H, Dieras V, Hegg R, Im SA, Shaw Wright G, et al: Atezolizumab and Nab-Paclitaxel in Advanced Triple-Negative Breast Cancer. N Engl J Med 2018, 379:2108-2121.
5. Monney L, Sabatos CA, Gaglia JL, Ryu A, Waldner H, Chernova T, Manning S, Greenfield EA, Coyle AJ, Sobel RA, et al: Th1-specific cell surface protein Tim-3 regulates macrophage activation and severity of an autoimmune disease. Nature 2002, 415:536-541.
6. de Mingo Pulido A, Gardner A, Hiebler S, Soliman H, Rugo HS, Krummel MF, Coussens LM, Ruffell B: TIM-3 Regulates CD103(+) Dendritic Cell Function and Response to Chemotherapy in Breast Cancer. Cancer Cell 2018, 33:60-74 e66.
7. Yan W, Liu X, Ma H, Zhang H, Song X, Gao L, Liang X, Ma C: Tim-3 fosters HCC development by enhancing TGF-beta-mediated alternative activation of macrophages. Gut 2015, 64:1593-1604.
8. Huang YH, Zhu C, Kondo Y, Anderson AC, Gandhi A, Russell A, Dougan SK, Petersen BS, Melum E, Pertel T, et al: CEACAM1 regulates TIM-3-mediated tolerance and exhaustion. Nature 2015, 517:386-390.
9. Zhou E, Huang Q, Wang J, Fang C, Yang L, Zhu M, Chen J, Chen L, Dong M: Up-regulation of Tim-3 is associated with poor prognosis of patients with colon cancer. Int J Clin Exp Pathol 2015, 8:8018-8027.
10. Ngiow SF, von Scheidt B, Akiba H, Yagita H, Teng MW, Smyth MJ: Anti-TIM3 antibody promotes T cell IFN-gamma-mediated antitumor immunity and suppresses established tumors. Cancer Res 2011, 71:3540-3551.

11. Andrews LP, Yano H, Vignali DA: Inhibitory receptors and ligands beyond PD-1, PD-L1 and CTLA-4: breakthroughs or backups. Nature immunology 2019:1-10.
12. Koyama S, Akbay EA, Li YY, Herter-Sprie GS, Buczkowski KA, Richards WG, Gandhi L, Redig AJ, Rodig SJ, Asahina H, et al: Adaptive resistance to therapeutic PD-1 blockade is associated with upregulation of alternative immune checkpoints. Nat Commun 2016, 7:10501.
13. Shan B, Man H, Liu J, Wang L, Zhu T, Ma M, Xv Z, Chen X, Yang X, Li P: TIM-3 promotes the metastasis of esophageal squamous cell carcinoma by targeting epithelial-mesenchymal transition via the Akt/GSK-3beta/Snail signaling pathway. Oncol Rep 2016, 36:1551-1561.
14. Feng ZM, Guo SM: Tim-3 facilitates osteosarcoma proliferation and metastasis through the NF-kappaB pathway and epithelial-mesenchymal transition. Genet Mol Res 2016, 15.
15. Zhang H, Song Y, Yang H, Liu Z, Gao L, Liang X, Ma C: Tumor cell-intrinsic Tim-3 promotes liver cancer via NF-kappaB/IL-6/STAT3 axis. Oncogene 2018, 37:2456-2468.
16. Zhuang X, Zhang X, Xia X, Zhang C, Liang X, Gao L, Ma C: Ectopic expression of TIM-3 in lung cancers: a potential independent prognostic factor for patients with NSCLC. Am J Clin Pathol 2012, 137:978-985.
17. Jiang J, Jin MS, Kong F, Cao D, Ma HX, Jia Z, Wang YP, Suo J, Cao X: Decreased galectin-9 and increased Tim-3 expression are related to poor prognosis in gastric cancer. PLoS One 2013, 8:e81799.
18. Yuan J, Jiang B, Zhao H, Huang Q: Prognostic implication of TIM-3 in clear cell renal cell carcinoma. Neoplasma 2014, 61:35-40.
19. Zhang Y, Cai P, Liang T, Wang L, Hu L: TIM-3 is a potential prognostic marker for patients with solid tumors: A systematic review and meta-analysis. Oncotarget 2017, 8:31705-31713.
20. Sun QY, Qu CH, Liu JQ, Zhang P, Yao J: Down-regulated expression of Tim-3 promotes invasion and metastasis of colorectal cancer cells. Neoplasma 2017, 64:101-107.
21. Wu J, Lin G, Zhu Y, Zhang H, Shi G, Shen Y, Dai B, Ye D: Low TIM3 expression indicates poor prognosis of metastatic prostate cancer and acts as an independent predictor of castration resistant status. Sci Rep 2017, 7:8869.
22. Zhang X, Yin X, Zhang H, Sun G, Yang Y, Chen J, Shu K, Zhao J, Zhao P, Chen N, et al: Differential expression of TIM-3 between primary and metastatic sites in renal cell carcinoma. BMC Cancer 2019, 19:49.
23. Cheng SQ, Han FY, Xu YQ, Qu T, Ju Y: Expression of Tim-3 in breast cancer tissue promotes tumor progression. International Journal of Clinical and Experimental Pathology 2018, 11:1157-1166.
24. Komohara Y, Morita T, Annan DA, Horlad H, Ohnishi K, Yamada S, Nakayama T, Kitada S, Suzu S, Kinoshita I, et al: The Coordinated Actions of TIM-3 on Cancer and Myeloid Cells in the Regulation of Tumorigenicity and Clinical Prognosis in Clear Cell Renal Cell Carcinomas. Cancer Immunol Res 2015, 3:999-1007.
25. Horlad H, Ohnishi K, Ma C, Fujiwara Y, Niino D, Ohshima K, Jinushi M, Matsuoka M, Takeya M, Komohara Y: TIM-3 expression in lymphoma cells predicts chemoresistance in patients with adult T-

cell leukemia/lymphoma. Oncol Lett 2016, 12:1519-1524.
26. Martin TA, Jordan N, Davies EL, Jiang WG: Metastasis to Bone in Human Cancer Is Associated with Loss of Occludin Expression. Anticancer Res 2016, 36:1287-1293.
27. Sasidharan Nair V, El Salhat H, Taha RZ, John A, Ali BR, Elkord E: DNA methylation and repressive H3K9 and H3K27 trimethylation in the promoter regions of PD-1, CTLA-4, TIM-3, LAG-3, TIGIT, and PD-L1 genes in human primary breast cancer. 2018, 10:78.
28. Tomkowicz B, Walsh E, Cotty A, Verona R, Sabins N, Kaplan F, Santulli-Marotto S, Chin C-N, Mooney J, Lingham RB: TIM-3 suppresses anti-CD3/CD28-induced TCR activation and IL-2 expression through the NFAT signaling pathway. PLoS One 2015, 10:e0140694.
29. Lee J, Su EW, Zhu C, Hainline S, Phuah J, Moroco JA, Smithgall TE, Kuchroo VK, Kane LP: Phosphotyrosine-dependent coupling of Tim-3 to T-cell receptor signaling pathways. Molecular and cellular biology 2011, 31:3963-3974.
30. Zhang H, Song Y, Yang H, Liu Z, Gao L, Liang X, Ma C: Tumor cell-intrinsic Tim-3 promotes liver cancer via NF-κB/IL-6/STAT3 axis. Oncogene 2018, 37:2456.
31. HeG K: NF-kappaBand STAT3-keyplayersin liverin-flammationand cancer. Cel Res 2011, 21:159-168.
32. Zhong Z, Wen Z, Darnell JE, Jr.: Stat3: a STAT family member activated by tyrosine phosphorylation in response to epidermal growth factor and interleukin-6. Science 1994, 264:95-98.
33. Gamero AM, Young HA, Wiltrout RH: Inactivation of Stat3 in tumor cells: releasing a brake on immune responses against cancer? Cancer Cell 2004, 5:111-112.
34. Huynh J, Chand A, Gough D, Ernst M: Therapeutically exploiting STAT3 activity in cancer - using tissue repair as a road map. Nat Rev Cancer 2019, 19:82-96.
35. Reilley MJ, McCoon P, Cook C, Lyne P, Kurzrock R, Kim Y, Woessner R, Younes A, Nemunaitis J, Fowler N, et al: STAT3 antisense oligonucleotide AZD9150 in a subset of patients with heavily pretreated lymphoma: results of a phase 1b trial. J Immunother Cancer 2018, 6:119.
36. Kettner NM, Vijayaraghavan S, Durak MG, Bui T, Kohansal M, Ha MJ, Liu B, Rao X, Wang J, Yi M: Combined inhibition of STAT3 and DNA repair in palbociclib-resistant ER-positive breast cancer. Clinical Cancer Research 2019.
37. Yang J, Liao X, Agarwal MK, Barnes L, Auron PE, Stark GR: Unphosphorylated STAT3 accumulates in response to IL-6 and activates transcription by binding to NFkappaB. Genes Dev 2007, 21:1396-1408.
38. Snyder M, Huang J, Huang XY, Zhang JJ: A signal transducer and activator of transcription 3.Nuclear Factor kappaB (Stat3.NFkappaB) complex is necessary for the expression of fascin in metastatic breast cancer cells in response to interleukin (IL)-6 and tumor necrosis factor (TNF)-alpha. J Biol Chem 2014, 289:30082-30089.
39. Banerjee K, Resat H: Constitutive activation of STAT3 in breast cancer cells: A review. Int J Cancer 2016, 138:2570-2578.
40. Leslie K, Lang C, Devgan G, Azare J, Berishaj M, Gerald W, Kim YB, Paz K, Darnell JE, Albanese C, et al: Cyclin D1 is transcriptionally regulated by and required for transformation by activated signal

transducer and activator of transcription 3. Cancer Res 2006, 66:2544-2552.

41. Nedeljkovic M, Tanic N, Dramicanin T, Milovanovic Z, Susnjar S, Milinkovic V, Vujovic I, Prvanovic M: Importance of Copy Number Alterations of FGFR1 and C-MYC Genes in Triple Negative Breast Cancer. J Med Biochem 2019, 38:63-70.
42. Lo HW, Hsu SC, Xia W, Cao X, Shih JY, Wei Y, Abbruzzese JL, Hortobagyi GN, Hung MC: Epidermal growth factor receptor cooperates with signal transducer and activator of transcription 3 to induce epithelial-mesenchymal transition in cancer cells via up-regulation of TWIST gene expression. Cancer Res 2007, 67:9066-9076.
43. Shang Y, Li Z, Li H, Xia H, Lin Z: TIM-3 expression in human osteosarcoma: Correlation with the expression of epithelial-mesenchymal transition-specific biomarkers. Oncol Lett 2013, 6:490-494.
44. Gonzalez-Mariscal L, Miranda J, Raya-Sandino A, Dominguez-Calderon A, Cuellar-Perez F: ZO-2, a tight junction protein involved in gene expression, proliferation, apoptosis, and cell size regulation. Ann N Y Acad Sci 2017, 1397:35-53.
45. Yun JH, Park SW, Kim KJ, Bae JS, Lee EH, Paek SH, Kim SU, Ye S, Kim JH, Cho CH: Endothelial STAT3 Activation Increases Vascular Leakage Through Downregulating Tight Junction Proteins: Implications for Diabetic Retinopathy. J Cell Physiol 2017, 232:1123-1134.
46. Ryu WI, Lee H, Bae HC, Jeon J, Ryu HJ, Kim J, Kim JH, Son JW, Imai Y, Yamanishi K, et al: IL-33 down-regulates CLDN1 expression through the ERK/STAT3 pathway in keratinocytes. J Dermatol Sci 2018, 90:313-322.
47. Chen YJ, You ML, Chong QY, Pandey V, Zhuang QS, Liu DX, Ma L, Zhu T, Lobie PE: Autocrine Human Growth Hormone Promotes Invasive and Cancer Stem Cell-Like Behavior of Hepatocellular Carcinoma Cells by STAT3 Dependent Inhibition of CLAUDIN-1 Expression. Int J Mol Sci 2017, 18.
48. Chidiac R, Zhang Y, Tessier S, Faubert D, Delisle C, Gratton JP: Comparative Phosphoproteomics Analysis of VEGF and Angiopoietin-1 Signaling Reveals ZO-1 as a Critical Regulator of Endothelial Cell Proliferation. Mol Cell Proteomics 2016, 15:1511-1525.
49. Doi Y, Yashiro M, Yamada N, Amano R, Noda S, Hirakawa K: VEGF-A/VEGFR-2 signaling plays an important role for the motility of pancreas cancer cells. Ann Surg Oncol 2012, 19:2733-2743.
50. Pawlus MR, Wang L, Hu CJ: STAT3 and HIF1alpha cooperatively activate HIF1 target genes in MDA-MB-231 and RCC4 cells. Oncogene 2014, 33:1670-1679.
51. Liu JF, Ma SR, Mao L, Bu LL, Yu GT, Li YC, Huang CF, Deng WW, Kulkarni AB, Zhang WF, Sun ZJ: T-cell immunoglobulin mucin 3 blockade drives an antitumor immune response in head and neck cancer. Mol Oncol 2017, 11:235-247.
52. Zhang X, Wu X, Zhang F, Mo S, Lu Y, Wei W, Chen X, Lan L, Lu B, Liu Y: Paclitaxel induces apoptosis of esophageal squamous cell carcinoma cells by downregulating STAT3 phosphorylation at Ser727. Oncol Rep 2017, 37:2237-2244.
53. Gao J, Shao Z, Yan M, Fu T, Zhang L, Yan Y: Targeted regulationof STAT3 by miR-29a in mediating Taxol resistance of nasopharyngeal carcinoma cell line CNE-1. Cancer Biomark 2018, 22:641-648.

54. Fan Z, Cui H, Yu H, Ji Q, Kang L, Han B, Wang J, Dong Q, Li Y, Yan Z, et al: MiR-125a promotes paclitaxel sensitivity in cervical cancer through altering STAT3 expression. Oncogenesis 2016, 5:e197.
55. Huang WL, Yeh HH, Lin CC, Lai WW, Chang JY, Chang WT, Su WC: Signal transducer and activator of transcription 3 activation up-regulates interleukin-6 autocrine production: a biochemical and genetic study of established cancer cell lines and clinical isolated human cancer cells. Mol Cancer 2010, 9:309.
56. Burugu S, Gao D, Leung S, Chia SK, Nielsen TO: TIM-3 expression in breast cancer. Oncoimmunology 2018, 7:e1502128.
57. Byun KD, Hwang HJ, Park KJ, Kim MC, Cho SH, Ju MH, Lee JH, Jeong JS: T-Cell Immunoglobulin Mucin 3 Expression on Tumor Infiltrating Lymphocytes as a Positive Prognosticator in Triple-Negative Breast Cancer. J Breast Cancer 2018, 21:406-414.

Figures

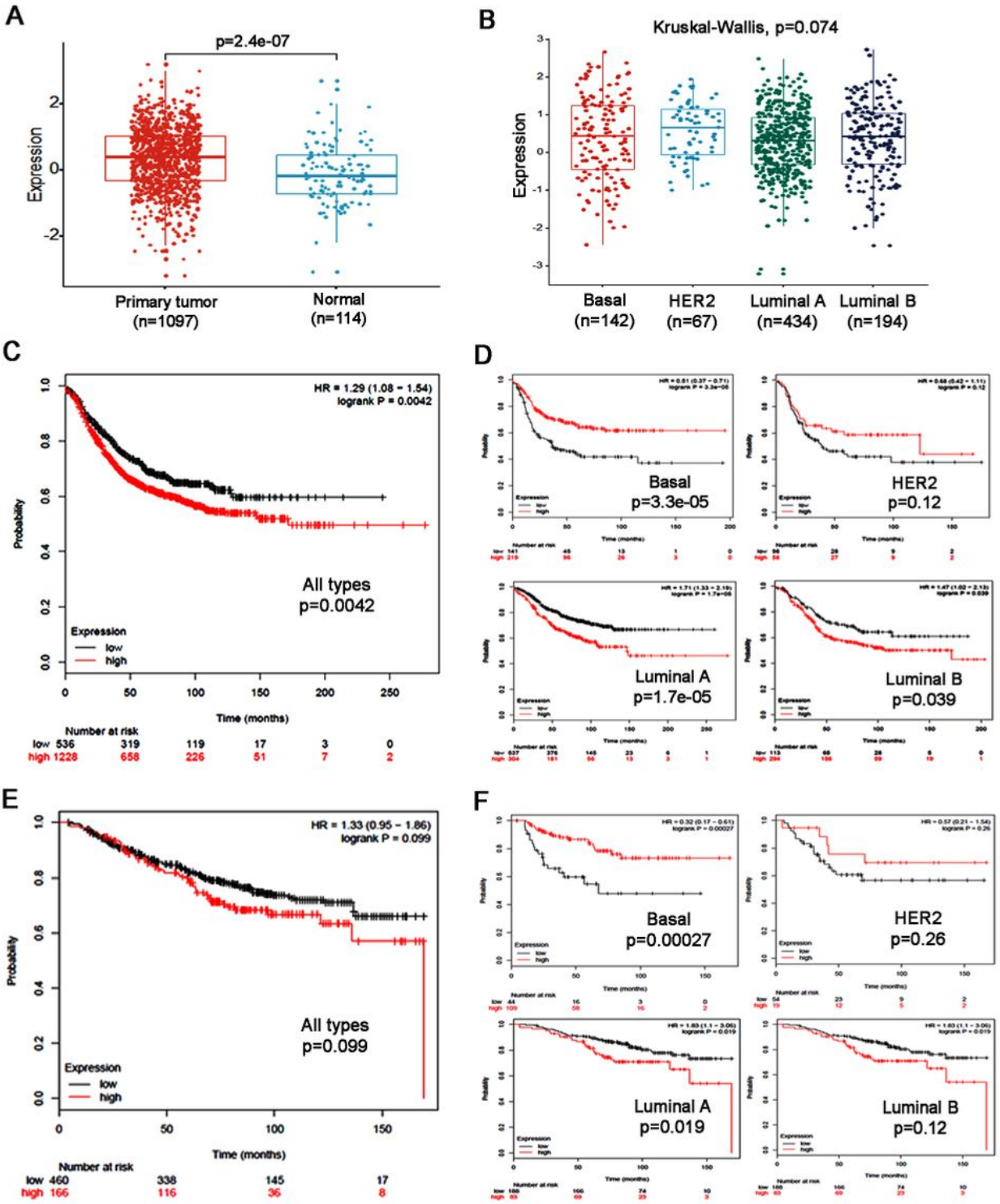

Figure 1

Gene expression level of Tim-3 on breast cancer and its association with patient survival. (A) Gene expression level of Tim-3 in the primary tumour vs. normal tissue (p<0.001). (B) Gene expression levels of Tim-3 among the breast cancer subgroups (p=0.074). (C) Association of the high level of the Tim-3 gene expression with poor RFS in overall breast cancer patients (p=0.004). (D) Association of the Tim-3 gene expression level with RFS among the subtypes of breast cancer. (E) Association of the high level of the

Tim-3 gene expression with poor OS in overall breast cancer patients. (F) Association of the Tim-3 gene expression level with OS among the subtypes of breast cancer.

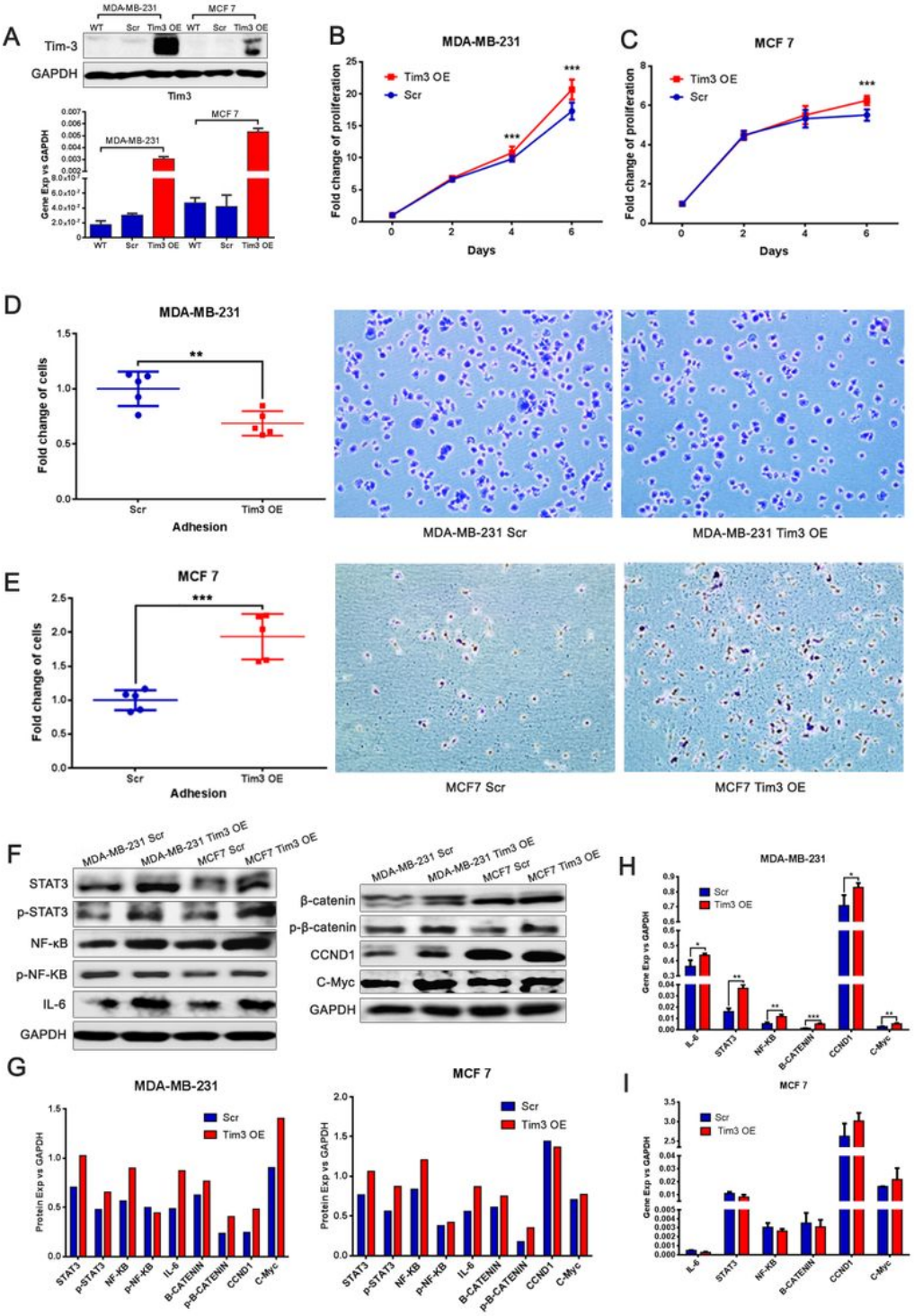

Figure 2

Effect of Tim-3 overexpression on the proliferation, adhesion and signalling pathway of the breast cancer cells. (A) Validation of the overexpression of Tim-3 in MDA-MB-231 and MCF7 cells by q-PCR and Western blot. (B) Effect of Tim-3 overexpression on cell proliferation of MDA-MB-231 cells (6 days,

p<0.001). (C) Effect of Tim-3 overexpression on cell proliferation of MCF7 cells (6 days, p<0.001). (D) Tim-3 overexpression reduced the adhesive ability in MDA-MB-231 cells (p=0.006). (E) Effect of Tim-3 overexpression on the adhesive ability in MCF7 cells (p<0.001). (F) Protein level of STAT3, phosphorylated STAT3, NF-κB, phosphorylated NF-κB, IL-6 and proliferative proteins in cells assessed by Western blot. (G) Quantitative densitometric analysis of the Western blot (n=3) using Image J software. (H) Gene expression profile in the MDA-MB-231 cell line. (I) Gene expression profile in the MCF7 cell line (n=3).

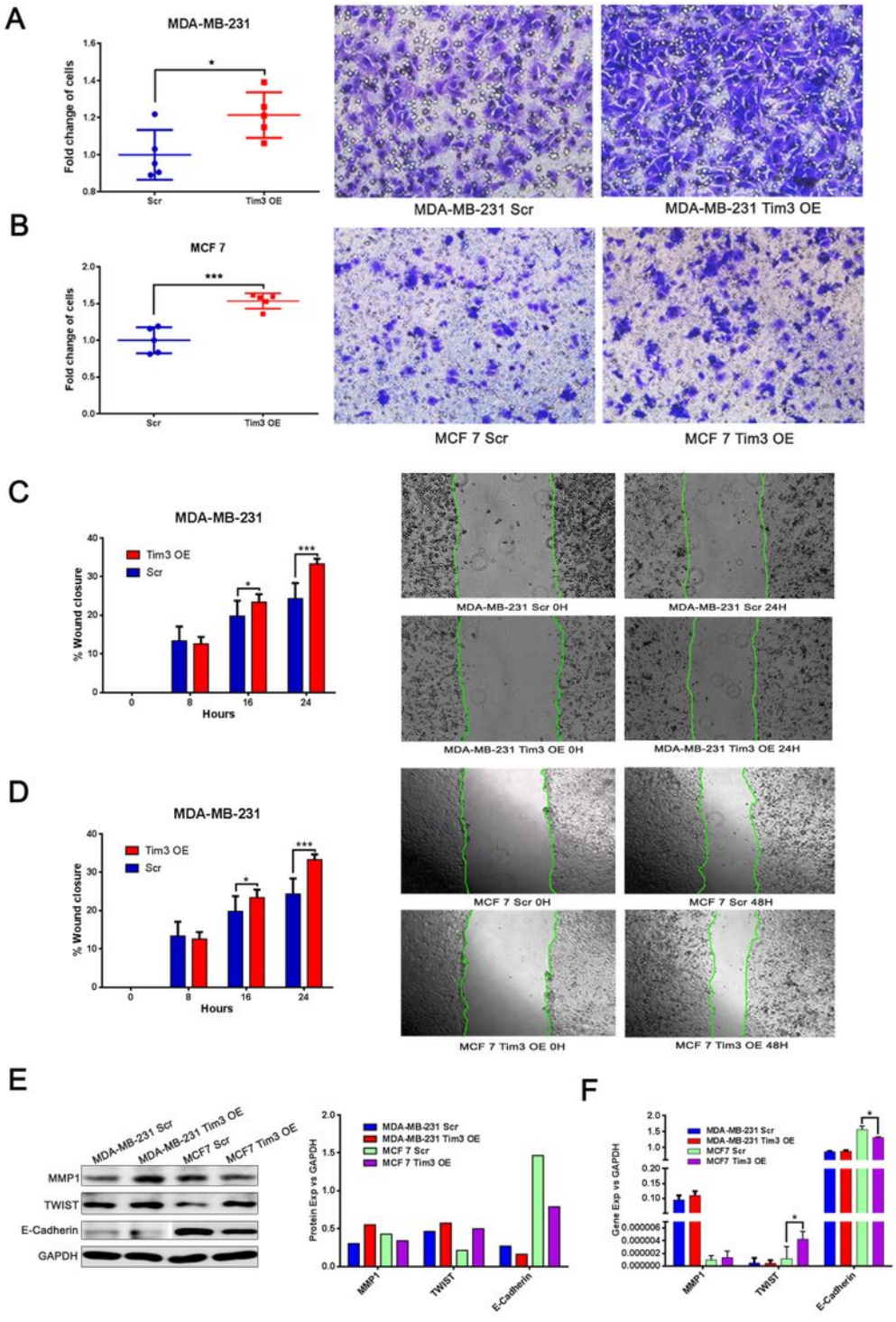

Figure 3

Effect of Tim-3 overexpression on invasion and migration of breast cancer cells in vitro. (A) Invasive ability in MDA-MB-231 cells after Tim-3 overexpression. (B) Invasive ability in MCF7 cells after Tim-3 overexpression. (C) Wound healing migration ability of MDA-MA-231 Tim3 OE cells. (D) Wound healing migration ability of MCF7 Tim3 OE cells. (E) Protein levels of MMP1, TWIST and E-cadherin in the breast cancer cells assessed by Western blot (left) and quantitative densitometric analysis of the intensity (n=3. right). (F) Gene expression levels of MMP1, TWIST and E-cadherin in the Tim3 OE and Scr cells assessed by qRT-PCR (n=3).

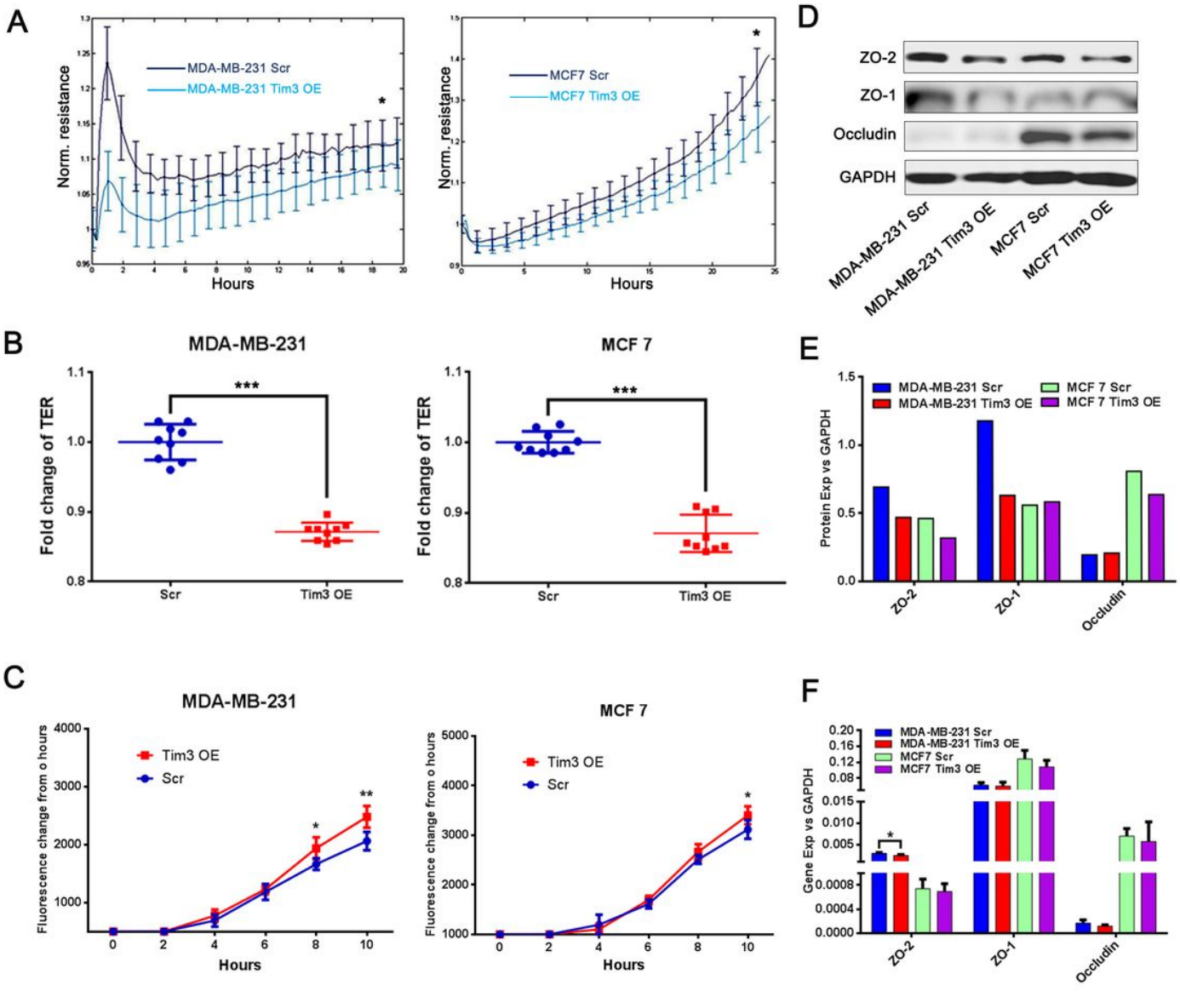

Figure 4

Role of Tim-3 in tight junction function in breast cancer cells. (A) Decelerated cell initial attachment and spreading in both MDA-MB-231 and MCF7 cell lines after Tim-3 overexpression assessed by ECIS. (B)

Effect of Tim-3 overexpression on TER in both MDA-MB-231 and MCF7 cell lines. (C) Effect of Tim-3 overexpression on the permeability between cells monolayers in MDA-MB-231 and MCF7 cell lines. (D) Protein levels of ZO-2, ZO-1 and Occludin in the Scr and Tim3 OE cells assessed by Western blot. (E) Quantitative densitometric analysis of Western blot using Image J software. (F) mRNA expression levels of the ZO-2, ZO-1 and Occludin genes in the cell lines determined by qRT-PCR.

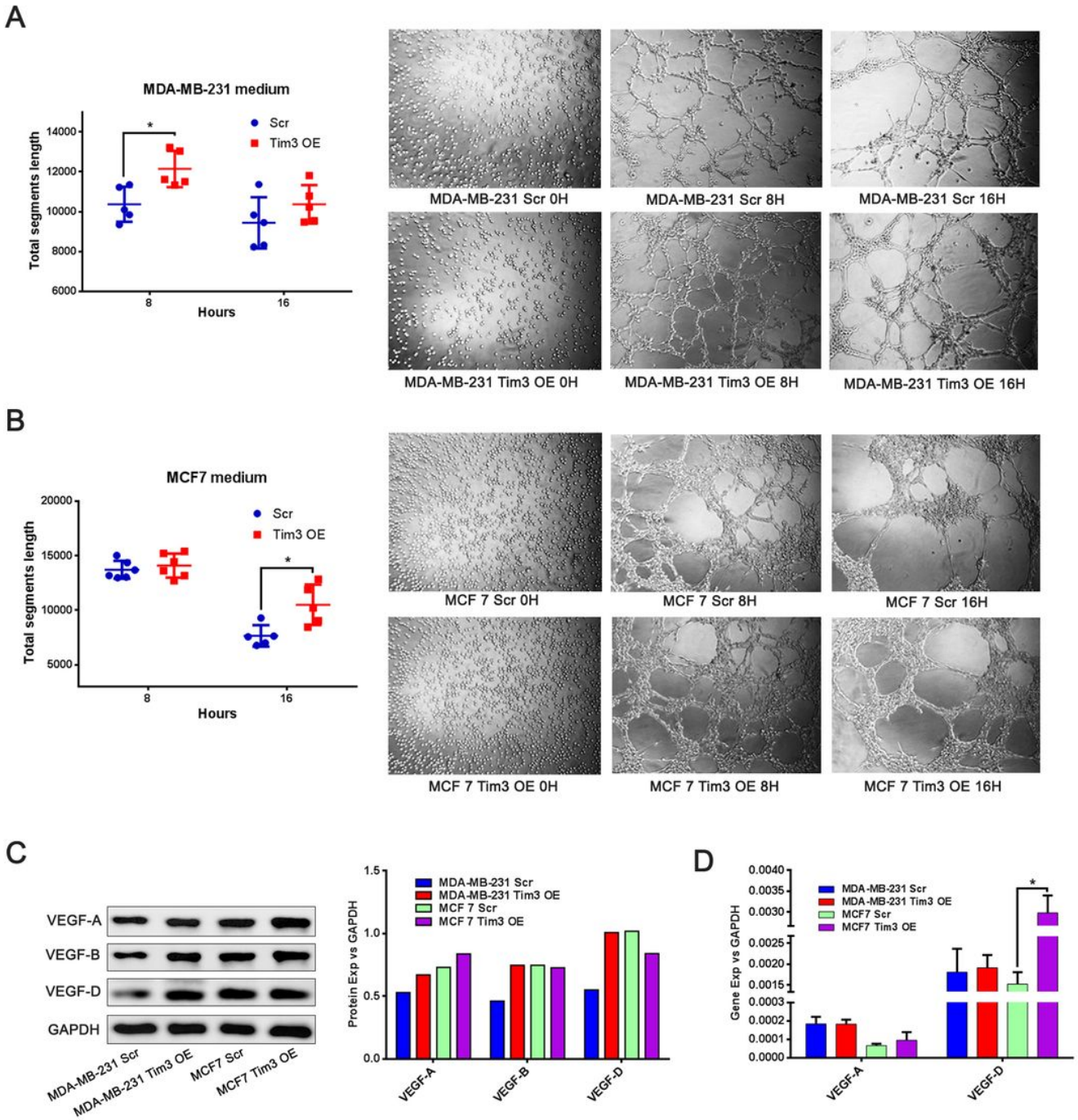

Figure 5

Effect of Tim-3 overexpression in cancer cells on tube formation of endothelial cells. (A) Tube formation ability of HUVECs cultured in conditioned medium from MDA-MB-231 Tim3 OE cells (p=0.014 vs Scr). (B)

Tube formation ability of HUVECs cultured in conditioned medium from MCF7 Tim3 OE cells (*p=0.016 vs Scr). (C) Protein levels of VEGFA, VEGFB and VEGFD in the Scr and Tim3 OE cells indicated by Western Blot (left) and quantitative densitometric analysis (right). (D) mRNA expression of VEGFA and VEGFD genes in the breast cancer cells determined by qRT-PCR.

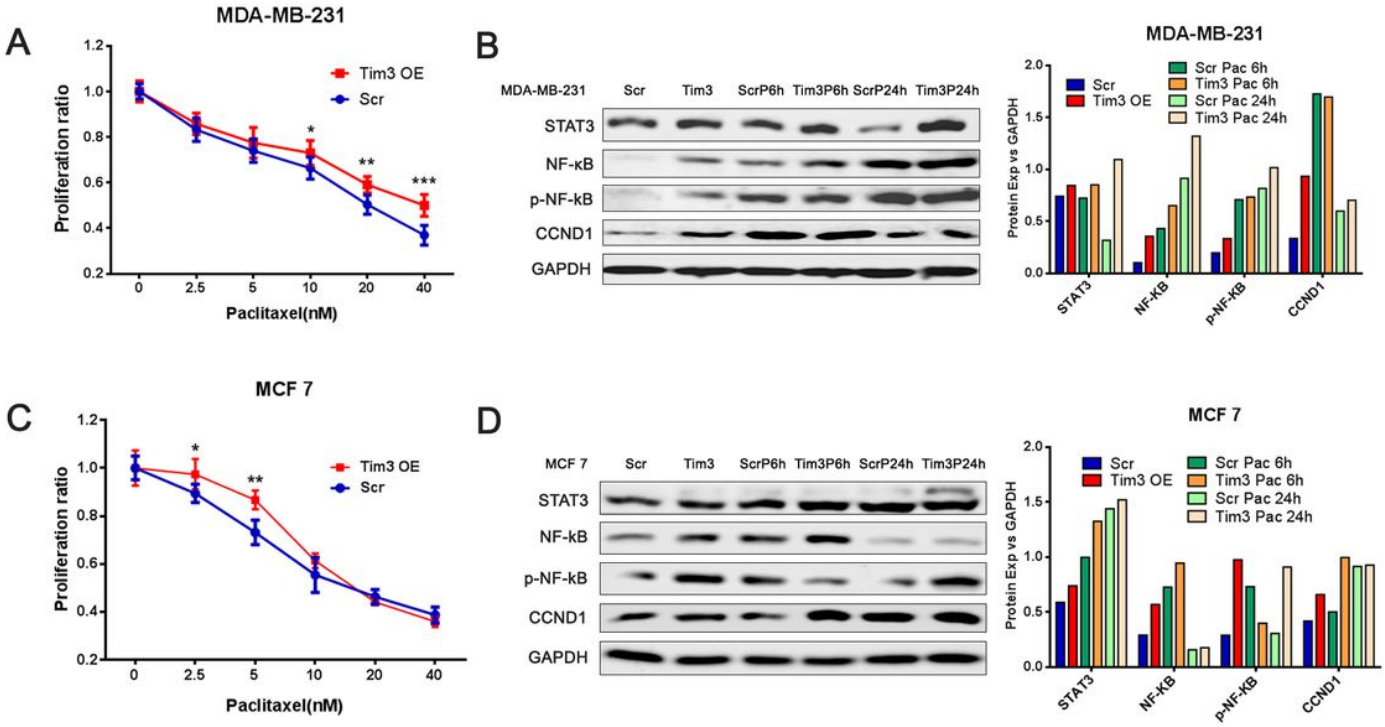

Figure 6

Effect of Tim-3 overexpression on the paclitaxel resistance in MDA-MB-231 and MCF7 cells. (A) Paclitaxel resistance in MDA-MB-231 cells indicated by the Alamar Blue cytotoxicity assay. Two-way ANOVA was used to evaluate the significance by considering two factors, paclitaxel doses and cell lines. Pairwise comparison between two cell lines was performed using the the Holm's post-hoc method. (B) Protein levels of STAT3, NF-κB, p-NF-κB and CCND1 in MDA-MB-231 cells treated with 10 nM paclitaxel as identified by Western blot (left), and the quantitative densitometry analysis. (C) Paclitaxel resistance in MCF7 cells indicated by the Alamar Blue cytotoxicity assay. Two-way ANOVA was used to evaluate the significance by considering two factors, paclitaxel doses and cell lines. Pairwise comparison between two cell lines was performed using the the Holm's post-hoc method. (D) Protein levels of STAT3, NF-κB, p-NF-κB and CCND1 assessed by Western blot in MCF7 cells treated with 5 nM paclitaxel as identified by Western blot (left) and quantitative densitometry analysis accordingly (right).

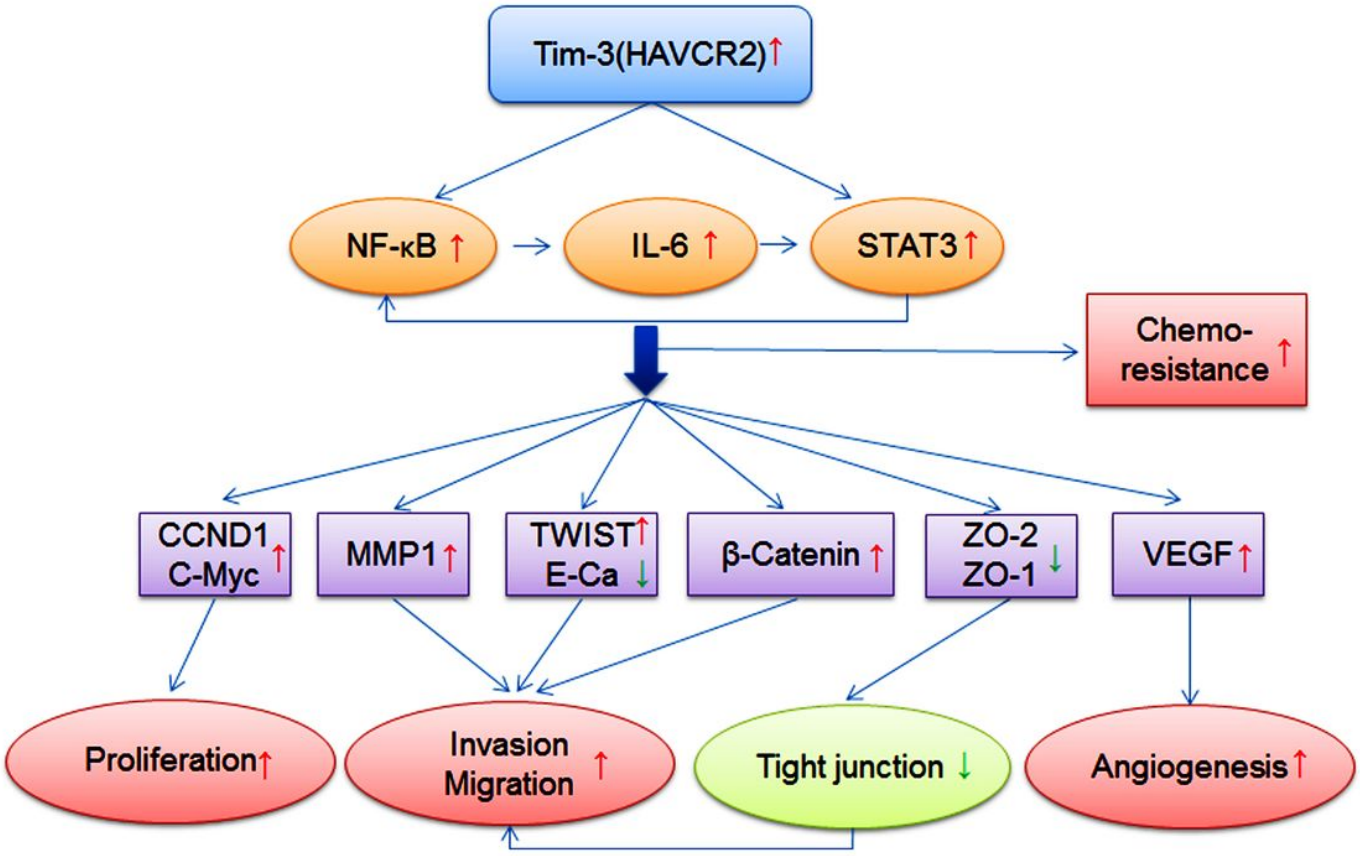

Figure 7

Schematic illustration of the role of Tim-3 in breast cancer. In brief, Upregulation of Tim-3 not only promotes cells proliferation, migration and invasion, but also disrupts cell-cell tight junction, increases angiogenesis of endothelial cells and paclitaxel-resistance. Tim-3 functions in breast cancer cells by activating NF-κB/STAT3 pathway and the following downstream genes.

Supplementary Files

This is a list of supplementary files associated with this preprint. Click to download.

- Sup.Fig.1.jpg
- Sup.Fig.2.jpg
- Sup.Fig.3.jpg
- Sup.Fig.4.jpg
- Sup.Fig.5.jpg